On the Accuracy of Time Domain Extension Formulae of Core Losses in Non-Oriented Electrical Steel Laminations under Non-Sinusoidal Excitation

Natheer Alatawneh[1*], Tanvir Rahman[2], Sajid Hussain[2], David A. Lowther[2], Richard Chromik[1]

1Department of Mining and Materials Engineering, McGill University, Montreal, Canada
2Department of Electrical and Computer Engineering, McGill University, Montreal, Canada
[*]natheer80@yahoo.com

Abstract: This paper presents a comparative study on the accuracy of three iron loss prediction models. The models are based on the decomposition of core or iron losses into the hysteresis and the eddy current loss components. The time domain extensions of two frequency domain models have been used to predict the iron losses due to a number of non-sinusoidal waveforms with and without the presence of minor loops. A third model, by Boglietti, that has been proposed recently to predict core losses for non-sinusoidal and Pulse Width Modulated (PWM) waveforms has also been studied. The unknown coefficients of each model have been determined by data fitting iron losses obtained from Epstein frame experiments for induction levels and fundamental frequencies up to 1.6 Tesla and 2 kHz, respectively. Core losses due to PWM waveforms have been measured at various fundamental and switching frequencies in unipolar and bipolar modes. The experimentally measured iron losses have been compared to those predicted using the three models and the accuracy and applicability of each model have been discussed.

1. Introduction

The accurate prediction of core losses in electromagnetic (EM) devices has been an area of active research for many decades. It is a crucial aspect of developing the next generation of highly efficient electromagnetic devices as well as for their optimization. Therefore, a great deal of research has been carried out to understand the iron loss phenomenon and develop loss prediction models to predict their values with increasing accuracy. The understanding of iron loss mechanisms and the accuracy of prediction models have improved over the years. From Steinmetz's original formula [1], much progress has been made on the development and application of empirical approaches for core loss predictions [2-4]. In addition to various empirical approaches, physics based phenomenological models such as the Jiles-Atherton and the Preisach model have also been developed [5] to calculate iron losses. Although superior to empirical approaches from the perspective of accuracy, the phenomenological models are computationally expensive and numerically unstable for integration into commercial Finite Element Analysis (FEA) solvers [6-8] at this point. Therefore, the empirical approaches remain the method of choice for calculating iron losses in most commercial and research applications. In this approach, the core losses in electromagnetic (EM) devices are calculated as a post-processed step. The flux density waveforms at each node of an FEA model is extracted (after quasi-static or transient solutions) and the losses are calculated by using the time domain versions of frequency domain empirical formulae [9]. Although these methods have been applied extensively to calculate losses in EM devices, to date, no direct comparison of their accuracy with experimental measurements for arbitrary, non-sinusoidal waveforms have been reported. This is quite remarkable given the ubiquity of their applications. In this research, the accuracy of a number of modern iron loss prediction formulae have been calculated for non-sinusoidal magnetizing waveforms and compared to experimental measurements.

Empirical iron loss models contain unknown parameters that are generally determined by mathematically fitting loss data from industry standard apparatus such as the Epstein frame, the Single Sheet Tester, or Toroids. A summary of these loss measurement methods and a review of some modern loss prediction models can be found in [10-12]. At present, the Epstein frame tester is recognized as the industry standard instrument for measuring iron losses of magnetic materials [13, 14]. In a typical Epstein frame, lamination samples are subjected to sinusoidal magnetizing waveforms at various frequencies and induction levels and the resulting losses are measured. The measured data are fitted to so-called frequency domain models whose accuracies are measured on the basis of R^2 values of the best fit models [3]. Although the standard practice is to apply sinusoidal waveforms to the Epstein frames, non-sinusoidal and PWM waveforms may also be applied if the hardware facilities allow for it. Empirical loss prediction models are generally expressed as a function of the magnetizing waveform frequency and the peak induction level under the assumption of sinusoidally varying waveforms. On the other hand, realistic waveforms in rotating electrical machines are typically: a) non-sinusoidal b) may contain minor loops due to PWM waveforms, and c) vectorial in nature. Characterization of the flux waveforms as a vector is posited on the basis that the tangential and radial flux components (or *x* and *y* components) are out of phase in the time domain and varies with position within a device. It is well established in literature that the vector fields produce rotational core losses which are fundamentally different from the well-known pulsating core losses [15, 16] studied here. Vectorial flux pattern may or may not be associated with minor loops, *i.e*. if one or both of the radial and tangential components have minor loops then the associated major hysteresis loop contain minor loops [17].

Given that realistic flux density waveforms are non-sinusoidal, frequency domain empirical models have to be extended to the time domain for calculating the iron losses in real devices. The extension of frequency domain models to the time domain is non-trivial. A great deal of research has been carried out over the years on this subject and a number of methodologies have been proposed [3, 18]. Each of these methodologies include various underlying assumptions but in the limit of sinusoidal magnetizing waveforms, the time domain models are required to reproduce the losses predicted by the frequency domain models.

In this research, in order to assess the accuracy of some modern iron loss formulae, their time domain versions have been used to predict the iron losses for magnetizing waveforms generated using triangular, trapezoidal and square voltage waveforms. In addition, losses due to PWM waveforms have also been measured and predicted using these formulae. The results of these computations have allowed for direct comparisons to be made on the accuracy of various models as well as their range of applicability with respect to waveform frequencies and the induction levels. These results will help formulate the next generation of computationally efficient iron loss prediction models.

The reminder of this paper is organized as follows. Section 2 presents the empirical frequency domain models that have been used in this study. The time domain extensions of the considered frequency domain models are discussed in section 3. A detailed description of the experimental approach and measurement results are presented in section 4. Finally, section 5 provides some final conclusions that assess the accuracy and the applicability of the models for various non-sinusoidal excitations.

2. Frequency Domain Loss Prediction Models

The classical Steinmetz equation [1] was the first iron loss formula proposed in 1894. Since then the equation has been modified and extended to include various loss components which reflect modern understanding of the physical mechanisms that leads to iron losses [2-4]. Many of the frequency domain models have also been extended to the time domain for predicting losses due to arbitrary flux density waveforms [19, 20]. Most modern effort towards extending frequency domain models into the time domain have been applied to loss separation models which divide the losses into two main components, the hysteresis loss, P_h, and the eddy current loss, P_e. In [21], Bertotti introduced a third loss component called the excess or anomalous loss that is a function of the material micro-structure, the conductivity, and the cross sectional area of the lamination. The three term Bertotti model has been studied extensively and it is one of the main iron loss prediction models that has been considered in engineering applications. However, in this work, the two term models will be studied for a number of reasons. First, most commercial FEM software packages apply various versions of the two term model only. In these models a global eddy current loss component is defined which combines the effects of the excess and the classical losses. This is a valid approach even though the excess loss of the Bertotti model and the classical eddy current losses have different frequency exponents. This is because the variation of the two term model parameters, k_e, k_h, $k_{h\alpha}$, and α (defined below) with respect to the frequency and induction levels take into account the behavioral differences that arise from the different exponents [2, 21-23]. Second, the three term model remains controversial in the iron loss research community with respect to its inclusion in iron loss models on the basis of physical principles. As it stands, it is attributed to losses that cannot be accounted for by the classical hysteresis and eddy current loss mechanisms. The validity of this approach is not universally accepted and this provides another reason for considering the two term models only. Third, a practical reason for studying the two term models is that most steel manufacturers usually provide loss data based on the two component assumption. A summary of the two term frequency domain models studied in this research have been given below.

In [24], Jordan introduced the first two term core loss model in which both the hysteresis and the eddy current loss components depend on the squared peak flux density. Jordan's core loss formula is given by,

$$P_c = k_h B^2 f + k_e B^2 f^2 \tag{1}$$

Where B is the peak flux density of a sinusoidal waveform, f is the frequency, k_h and k_e are the hysteresis and eddy currents coefficients, respectively. Eq. (1) represents the simplest form of modern frequency domain formulae for iron losses. To better reflect the non-linear behavior of the hysteresis loss component, an improved formulation was proposed by [25] in which the hysteresis component has been modified to be,

$$P_c = k_{h\alpha} B^\alpha f + k_e B^2 f^2 \tag{2}$$

In this formulation the exponent α is considered to be a polynomial function of the peak flux density at each frequency. Also, k_h(Eq. (1)) and k_e are functions of flux density $\boldsymbol{B}$ of a polynomial of order 3, while $k_{h\alpha}$(Eq. (2)) is considered to vary with frequency only. Eqns. (1) and (2) are designated as **Model A** and **Model B**, respectively. The aforementioned coefficients have been discussed in [25] and can be expressed as,

$$k_e = k_{e0} + k_{e1}B + k_{e2}B^2 + k_{e3}B^3 \tag{3}$$

$$k_h = k_{h0} + k_{h1}B + k_{h2}B^2 + k_{h3}B^3 \tag{4}$$

$$\alpha(B) = \alpha_0 + \alpha_1 B + \alpha_2 B^2 + \alpha_3 B^3 \tag{5}$$

α is calculated at each frequency, while $k_{h\alpha}$ can be extracted by considering the logarithmic operator as,

$$\log \frac{P_h}{f} = \log k_{h\alpha} + (\alpha_0 + \alpha_1 B + \alpha_2 B^2 + \alpha_3 B^3) \log B \tag{6}$$

Detailed algorithms for the model parameter identification have been discussed in [25].

3. Time Domain Extension Models

As mentioned above the frequency domain models of core losses presented in section 2 are valid for sinusoidal excitations only. Therefore, it is necessary to extend the frequency domain models to the time domain. The main idea behind this extension is to introduce an equivalent formula as a function of the rate of change of the flux density, *dB/dt*. Using this approach the eddy current loss component in the time domain can be written as [2],

$$P_e = \frac{1}{2T\pi^2}\int_0^T k_e(f_1, B)\left[\frac{dB(t)}{dt}\right]^2 dt \quad (7)$$

The hysteresis component for Model A is given by,

$$P_h = \frac{1}{2T}\int_0^T k_h(f_1, B)\left|B(t)\left[\frac{dB(t)}{dt}\right]\right| dt \quad (8)$$

The hysteresis component for Model B is given by,

$$P_{h\alpha} = \frac{\alpha\, k_{h\alpha}(f_1)}{4}\int_0^T \left|B(t)^{\alpha\,(B,f)-1}\left[\frac{dB(t)}{dt}\right]\right| dt \quad (9)$$

The accuracy of the models shown in Eqns. (7)-(9) have been studied in this research by using them to predict iron loss due to generalized waveforms. A third model considered in this study was developed by Boglietti *et. al*. and presented in [21] (henceforth referred to as the Boglietti model). This approach is also based on the two term iron loss decomposition. The unique aspect of the Boglietti model is that it was developed to predict losses due to PWM waveforms. Another difference between the Boglietti and the aforementioned models (Models A and B) is that the unknown parameters of the Boglietti model requires knowledge of the supply voltage waveforms whereas this is not the case for Models A and B. The Boglietti model is given by,

$$P_c = \eta^{\alpha} P_{h,sin} + \chi^2 P_{e,sin} \quad (10)$$

where, $\eta = \frac{V_{av}}{V_{av,fund}}$, $\chi = \frac{V_{rms}}{V_{rms,fund}}$, V_{av} and V_{rms} are the rectified average and the root mean square voltages, respectively, of the PWM generated waveform that the EM device is subjected to. The subscript *fund* is related to the fundamental waveform that may be extracted using a Fourier series decomposition of a general waveform. The coefficient α has been defined in (5).

4. Experimental Measurements and Results

Experiments were carried out on non-oriented electrical steel samples of grade 35WW300 using a 100 turn Epstein frame from Brokhaus Measurements and its MPG 200 system [26]. The Epstein frame can generate a flux density between 0.001 T to 2.0 T depending on the quality of the electrical steel being tested. The maximum sample mass is 1 kg. The MPG 200 system can take measurements at frequencies ranging from 3 Hz to 20 kHz. The power supply can apply maximum current of 40 A, and 100 V to the primary windings. The material being tested, the 35WW300, is a commercial grade material that is by weight, 3.1% Silicon (Si) and 0.65% Aluminum (Al). The non-oriented designation refers to uniformly distributed magnetic domains with no preferred magnetization direction [27]. It is commonly used to fabricate cores of rotating electrical machines. The samples used in this study are rectangular with dimensions of 300 mm × 30 mm × 0.35 mm.

The Epstein frame tests using the 35WW300 samples were carried out under three magnetizing conditions. First, under sinusoidal excitations to identify the frequency domain models parameters. Second, for non-sinusoidal waveforms that do not have minor loops, and third, for PWM waveforms with different fundamental and switching frequencies. The results of these measurements are presented and discussed in the following subsections.

4.1 Sinusoidal Measurements

The samples were tested under sinusoidal excitations for a range of frequencies from 50 Hz to 2 kHz, and for flux density levels from 0.1 T up to 1.6 T. The Brockhaus MPG 200 system is equipped with a digital control system that preserves the form factor of the induced secondary voltage to be below 1.111±1% error level which meets the recommended IEC international standard [28]. The losses ([W/kg]) were measured as a function of flux density at each frequency. The coefficients of the frequency domain models (Models A and B) were found by data fitting the Epstein frame loss results from sinusoidal waveforms to Eqns. (1) and (2). The fitting process involves separation of loses into hysteresis and eddy current components. The loss separation has been accomplished based on the extrapolation method of [29]. The polynomial coefficients of k_e, k_h, $k_{h\alpha}$, and α with respect to the flux density at various frequency levels were obtained using Eqns. (3) to (6). Some of these results have been shown in Fig. 1. The results show that k_e is of the order of 10^{-5} (Fig. 1(a)) which is smaller than those of k_h(Fig. 1(b)) and $k_{h\alpha}$ (Fig. 1(d)). The trends and orders of these results matches those of similar calculations reported previously in [3] and [25]. The variations of α with respect to the frequency and induction levels (Fig. 1(c)) take into account the influence of the skin effect.

Using these results in Fig. 1(a-d), the measured core losses under sinusoidal excitations have been compared to those predicted by the time domain loss prediction Models A and B (Eqns. (7)-(9)). Figs. 2(a) and 3(b) show the errors between the measured and the predicted losses. The results show that Model A predicts the losses accurately at high frequencies (> 500 Hz) with errors between$\mp 5\%$, while the error increases to almost -20% at 100 Hz and low flux density levels. On the other hand, Model B predicts the losses fairly accurately (typically within$\mp 2\%$) for the entire range of flux density and supply frequencies. These results are similar to those reported previously [3]. An important conclusion of these results is that the time domain extended version of Eqns. (1) and (2) reproduce the expected levels of accuracy when applied to sinusoidal waveforms.

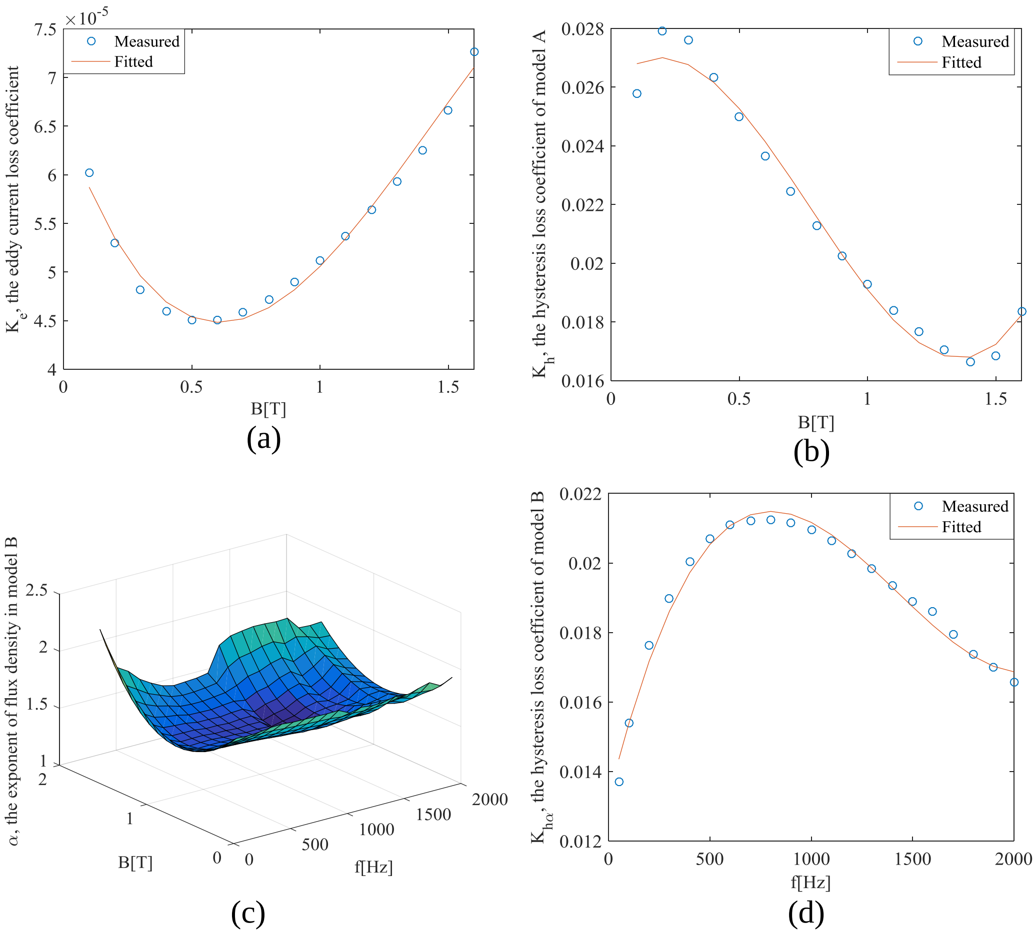

Fig. 1: *The unknown parameters of models A and B are calculated using the measurement results. (a) k_e is the eddy current loss coefficient for both A and B models. (b) k_h is the hysteresis loss coefficient of Model A. (c) α is the exponent coefficient of flux density in Model B. (d) $k_{h\alpha}$ is the hysteresis loss coefficient of Model B.*

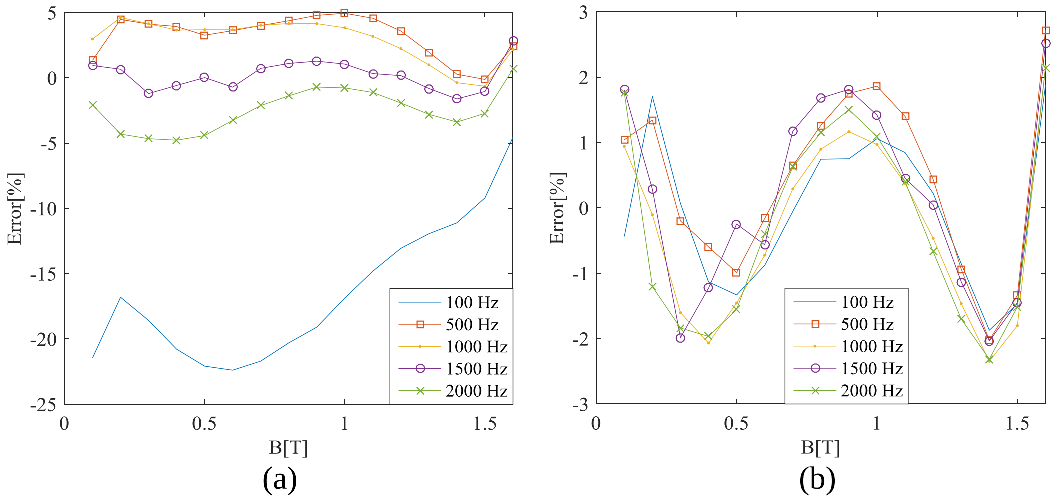

Fig. 2: *The percentage of relative errors between the measured and the calculated core losses under sinusoidal excitations at different frequencies and peak flux densities. Losses were calculated using (a) Model A (b) Model B.*

4.2 Non-Sinusoidal Measurements

Some non-sinusoidal voltage waveforms and the resulting losses are considered in this section. The waveforms and results presented below are for those that do not contain minor loops. Waveforms containg minor loops will be considered in the next subsection. The non-sinusoidal waveforms chosen for study are triangular, trapezoidal, and square shaped voltages including dead times. The Epstein frame was supplied with voltage signals corresponding to these shapes and the resulting flux density and core losses were measured. Loss measurements were taken at a number of frequencies and maximum induction levels. All three models discussed in section 3 were used to calculate the expected core losses and the relative errors between the measured and the time domain models were calculated using,

$$Error\ [\%] = \frac{P_{measured} - P_{predicted}}{P_{measured}} \times 100\ \% \tag{11}$$

Fig. 3 shows the results of losses due to the triangular-wave voltage excitations. Fig. 3 (a) shows an example triangular waveform at 50 Hz and the associated induced flux density waveform. In Fig. 3 (b), the relative errors between the measured and the predicted losses have been shown for the 50 Hz waveform as a function of peak flux density level for all three loss models. It is observed that Model B and the Boglietti model are in a good agreement with the experimental measurements with a relatively low percentage of error of less than 10%, while Model A errors range between -15 to -35 %. When the excitation frequency was increased to 300 Hz and 1500 Hz, as shown in Fig. 3 (c) and Fig. 3 (d), respectively, all three models predict the losses moderately accurately (between -5% to ~15%) with increasing frequency. This may be explained by considering the eddy current loss component, which increases as a power of two with frequency and that makes it dominant over the hysteresis loss component as frequency increases. Since the same time domain expression (Eqn. (7)) for eddy current loss component (which is known to be exact) is used in the three models, high accuracy levels are expected for all three models. Similar results have also been found for the trapezoidal and the square voltage waveforms as shown in Fig. 4 and Fig. 5, respectively. These results show that both the Boglietti Model and Model B give acceptable results for all ranges of frequencies while Model A is not reliable for low frequencies such as 50 Hz as the errors may be in excess of 30 %.

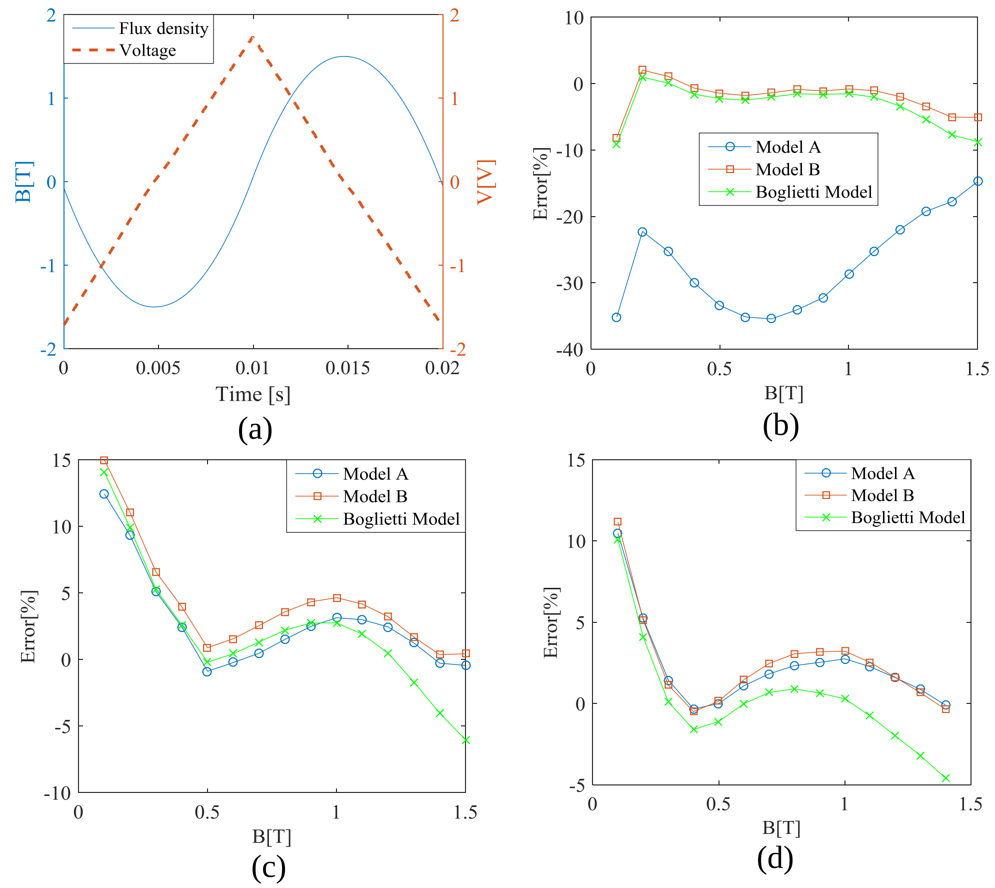

Fig. 3*: (a) The triangular-wave excitation voltage and its corresponding flux density waveform. (b) The relative error between predicted and measured losses as a function of flux density. Losses are predicted using time domain Model A, Model B, and Boglietti model with a triangular waveform at 50 Hz. (c) At 300 Hz. (d) At 1500 Hz.*

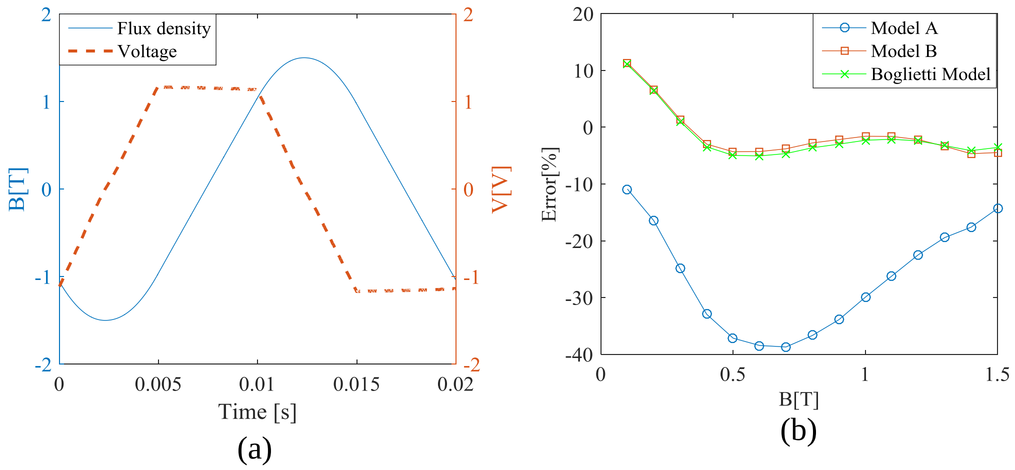

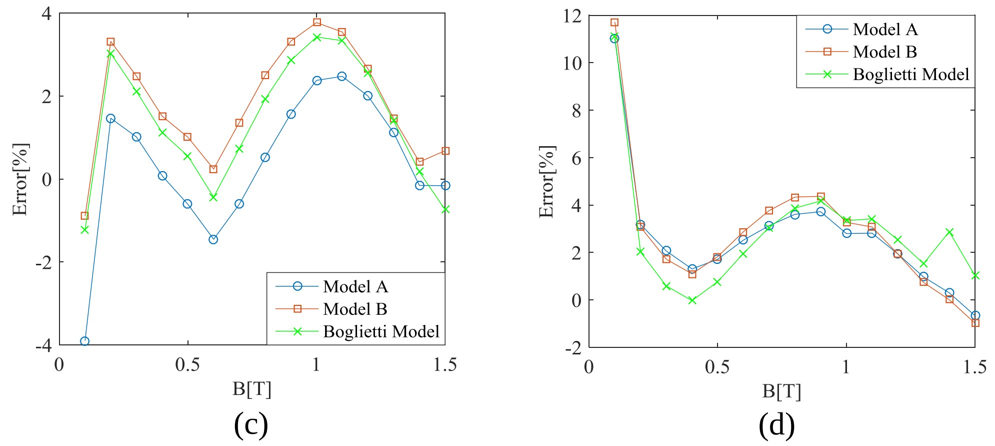

Fig. 4*: (a) The trapezoidal-wave excitation voltage and its corresponding flux density waveform. (b) The relative error between predicted and measured losses as a function of flux density. Losses are predicted using time domain Model A, Model B, and Boglietti model with a trapezoidal waveform at 50 Hz. (c) At 300 Hz. (d) At 1500 Hz.*

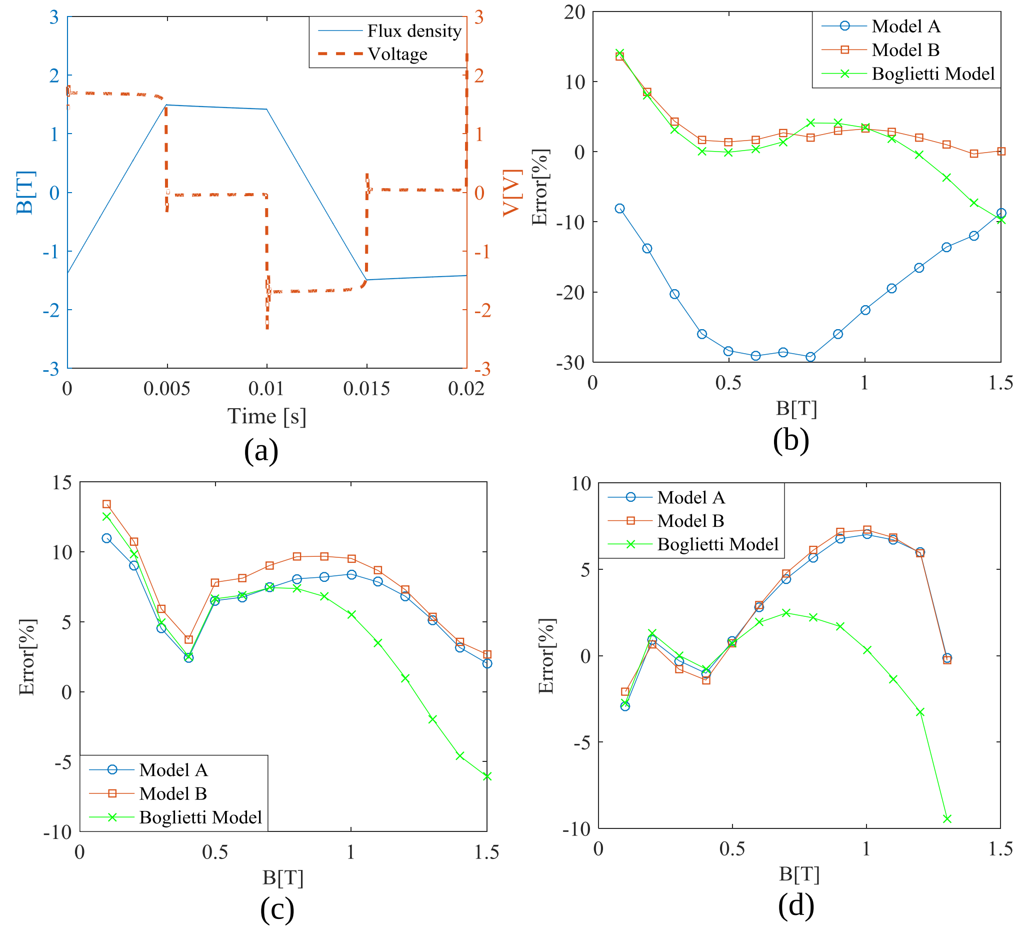

Fig. 5*: (a) The square waveform with dead time as an excitation voltage and its corresponding flux density waveform. (b) The relative error between predicted and measured losses as a function of flux density. Losses are predicted using time domain Model A, Model B, and Boglietti model with a square waveform at 50 Hz. (c) At 300 Hz. (d) At 1500 Hz.*

4.3 PWM Measurements

Pulse width modulation inverters are commonly used to control AC motors. Buck-boost, boost and buck converters and inverters are used to control the phase voltages by changing the voltage magnitude, the phase and the frequency. The use of PWM techniques offer several advantages such as controlling the harmonic content of phase currents and voltages that may be used to minimize the torque ripple and other parasitic effects in electric machines. A consequence of using PWM generated waveforms is that the machine cores are subjected to rapidly fluctuating magnetic fields (as opposed to an ideal sinusoidal or non-sinusoidal waveform) which may or may not contain minor loops. In this section, the accuracy of the loss models presented above is evaluated for PWM generated waveforms. PWM signals are usually generated in unipolar and bipolar modes. In the unipolar mode, the instantaneous value of the voltage pulse has the same sign as its fundamental harmonic. In the bipolar mode, the positive and the negative periods of the fundamental harmonic are generated using a combination of positive and negative pulses. Fig. 6 illustrates an example of bipolar and unipolar PWM waveforms.

Experimental tests using the Epstein frame were performed in unipolar and bipolar modes in this research. Loss measurements were taken at two fundamental frequencies (f_{fun}), 50 Hz and 400 Hz, that were generated using low and high switching frequencies (f_s), as shown in Table 1. For the 50 Hz fundamental, the low and high switching frequencies were 500 Hz and 3 kHz, respectively. For the 400 Hz fundamental, the low and the high switching frequencies were 4 kHz and 20 kHz, respectively. Before presenting and discussing the loss comparison results an important point has to be made regarding the core loss measurements at low induction levels (< ~0.1 T). Core losses are directly proportional to the peak flux density levels (Eqns. (1) and (2)). Therefore, at very low flux density levels, depending on the systematic error of the equipment the measured iron loss may well be of the order of the systematic error. In such cases, the errors between predicted and measured values may be unrealistically high and would not necessarily reflect the accuracy of the models being investigated. Because of this the relative errors at low flux density levels are excluded from the following analysis, as has been done previously in [23], where the relative errors between measured and predicted values have been presented between 0.4 T to 1.6 T.

The measured losses have been compared to those predicted by Models A, B and the Boglietti model and the relative errors have been computed. Fig. 7(a) shows the relative errors as a function of flux density in the unipolar mode for f_{fun} =50 Hz and switching frequency, f_s=500 Hz. The results show that Model B is fairly accurate with error levels ranging from ~2%-11%. Model A errors may be as high as ~25% compared to the measured losses. The relative errors for the Boglietti model ranges from ~20%- 50%. For the same fundamental and switching frequencies (f_{fun} =50 Hz and f_s=500 Hz) with the bipolar PWM scheme, Model B has the lowest error among the three models with a maximum error ~25%, as shown in Fig. 7(b). As the switching frequency is increased to 3 kHz, the accuracy of Model B decreases to errors of ~20 % (first three points are excluded). The accuracy of Model A decreases significantly with a maximum error of ~60%, while the Boglietti model's accuracy improves to ~15%- 22%, as shown in Fig. 7(c). For bipolar PWM at high switching frequency, 3kHz, all three models show high percentage of errors, higher than ~60%, as shown in Fig. 7(d). In summary, for PWM generated waveform at 50 Hz, Model B performs well for switching frequency f_s=500 Hz in unipolar mode. In addition, Model B is moderately accurate (see APPENDIX for definition of various accuracy designations) for f_s =500 Hz in bipolar mode and f_s =3 kHz, in unipolar mode. Model A is only moderately accurate at low switching frequency, *fs* =500 Hz with unipolar PWM. The Boglietti model performs well at high switching frequency, f_s =3 kHz in unipolar mode.

Some of these results would be significantly affected by the presence of high order harmonics, which are more pronounced in bipolar modes. Consider Fig. 8, which shows the major dynamic hysteresis loops due to a PWM waveform using the unipolar and the bipolar modes. It clearly shows the influence of the harmonics in bipolar mode due to the presence of minor loops. In general, the presence of minor loops deteriorate the accuracy of all three core loss models, and this decrease in accuracy is most significant for the Boglietti model. Consider now the accuracy of the models for the case of 400 Hz fundamental frequency. The results have been presented in Fig. 9. In Figs. 9(a) and 9(b), the model errors have been shown for unipolar and bipolar modes, respectively, at switching frequency f_s=4 kHz. Both models A and B show similar error levels ranging from ~5%-20%. The Boglietti model performs better under the unipolar scheme. In Figs. 9(c) and 9(d), similar results have been presented at f_s =20 kHz. At this frequency in bipolar mode, both models' errors exceed 20%. The Boglietti model predicts losses accurately for the unipolar scheme at both f_s =4 kHz and 20 kHz, while, in bipolar mode, the errors surpass 25% at f_s = 4 kHz and is between 30% to 50% at f_s =20 kHz. Besides these results, another observation is that the predicted losses using the Boglietti model generally underestimates the core loss in unipolar modes and overestimates it in bipolar modes. It is also important to point out that the Boglietti model assumes the absence of minor loops, which is reflected by its poor performance for bipolar schemes. In general, the two methods of switching, bipolar and unipolar, generate vastly different harmonic spectra. This causes the precisions of models A, B and the Boglietti model to vary significantly. Table 2 in the APPENDIX summarizes the accuracies of all presented models at various frequencies and PWM excitation schemes.

Table 1 The Properties of PWM Waveforms

f_{fun}[Hz]	f_s[Hz]	Scheme
50	500	UNI
		BI
	3 k	UNI
		BI
400	4 k	UNI
		BI
	20 k	UNI
		BI

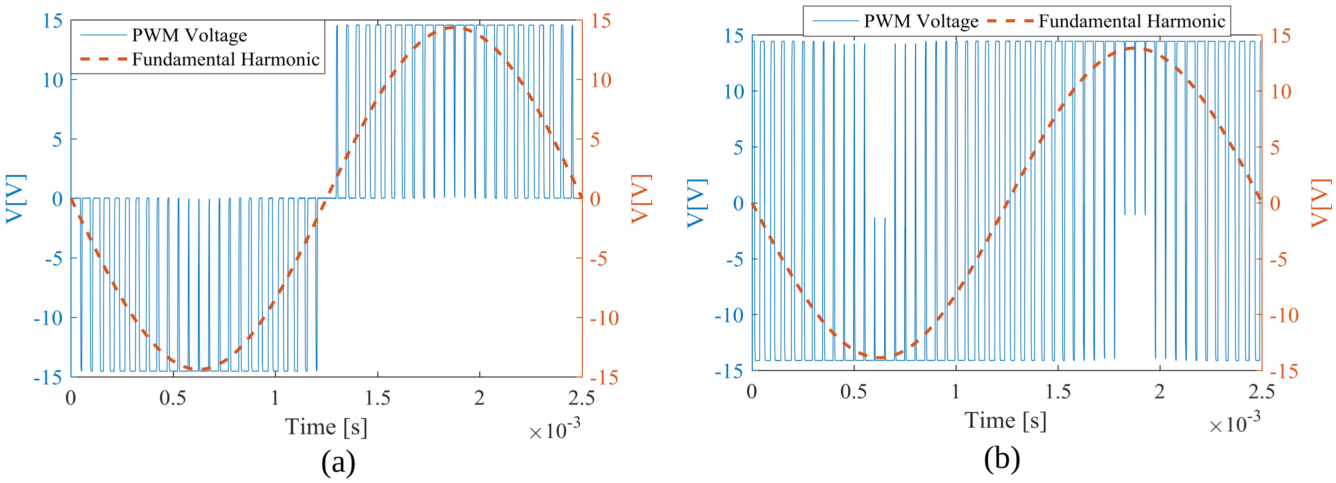

Fig. 6*: Measured PWM waveform at f_{fun}=400 Hz with the corresponding fundamental harmonic for (a) Unipolar mode (b) Bipolar mode*

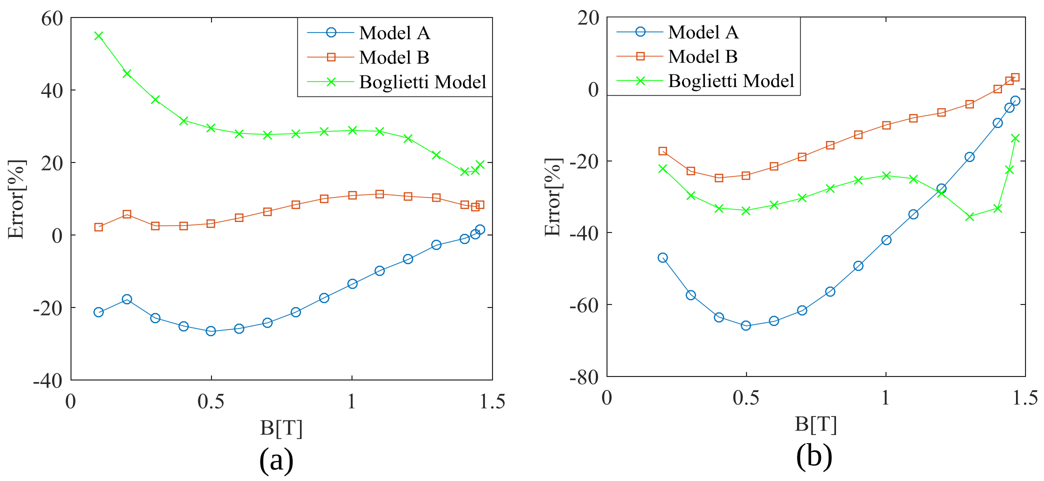

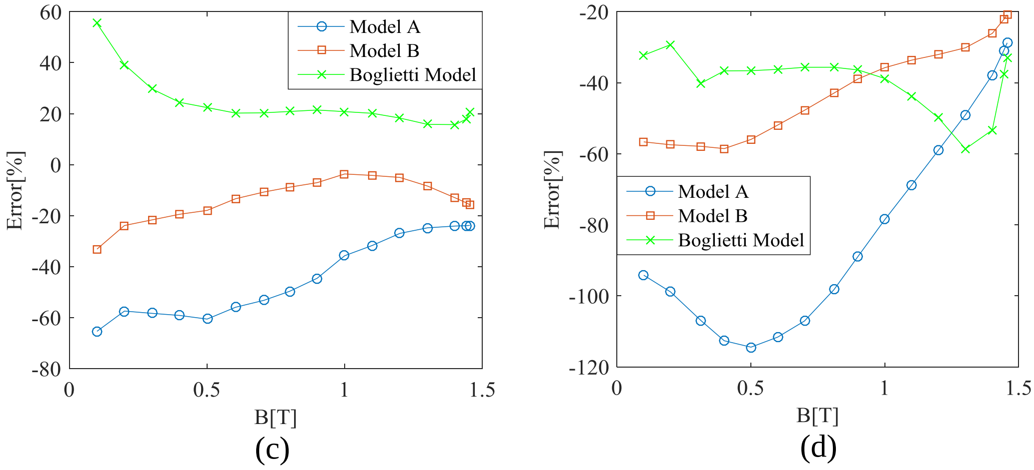

Fig. 7: *The relative error between predicted and measured losses as a function of flux density. Losses are predicted using time domain Model A, Model B, and Boglietti model with PWM waveform at f_{fun}=50 Hz and (a) Unipolar mode f_s=500 Hz (b) Bipolar mode f_s=500 Hz (c) Unipolar mode f_s=3k Hz (d) Bipolar mode f_s=3k Hz*

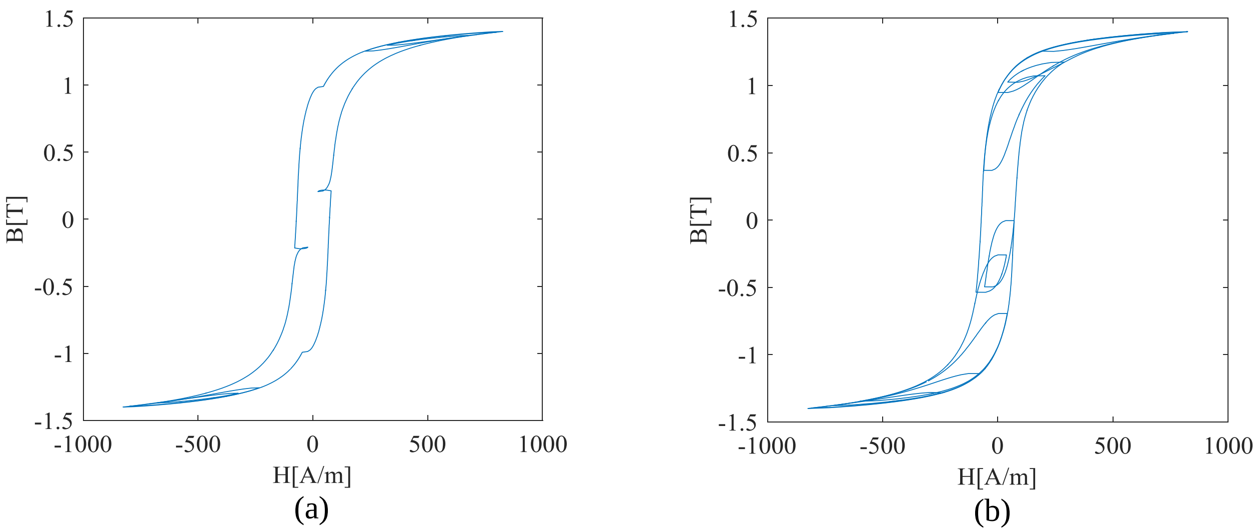

Fig. 8: *The dynamic hysteresis loops associated to the PWM supply at f_{fun} =50Hz and f_s=500 Hz for (a) Unipolar mode (a) Bipolar mode*

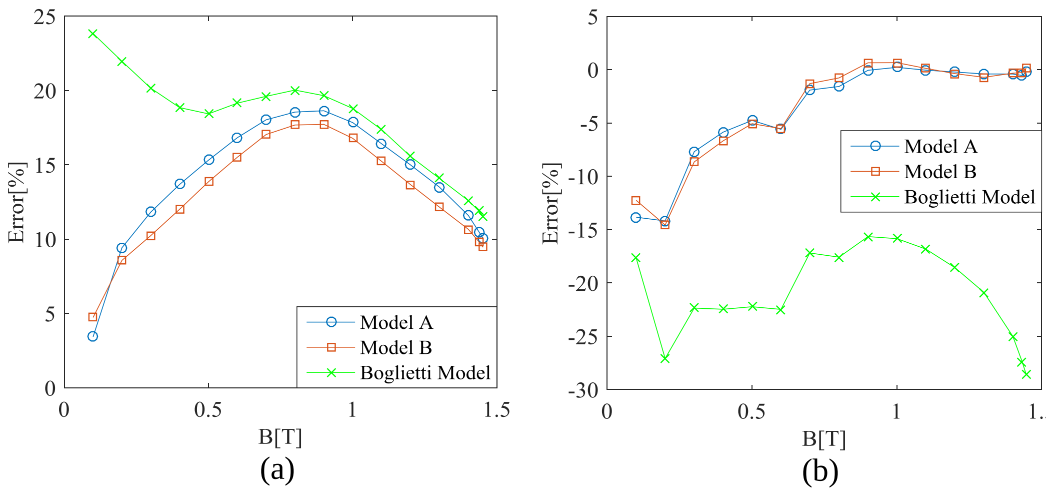

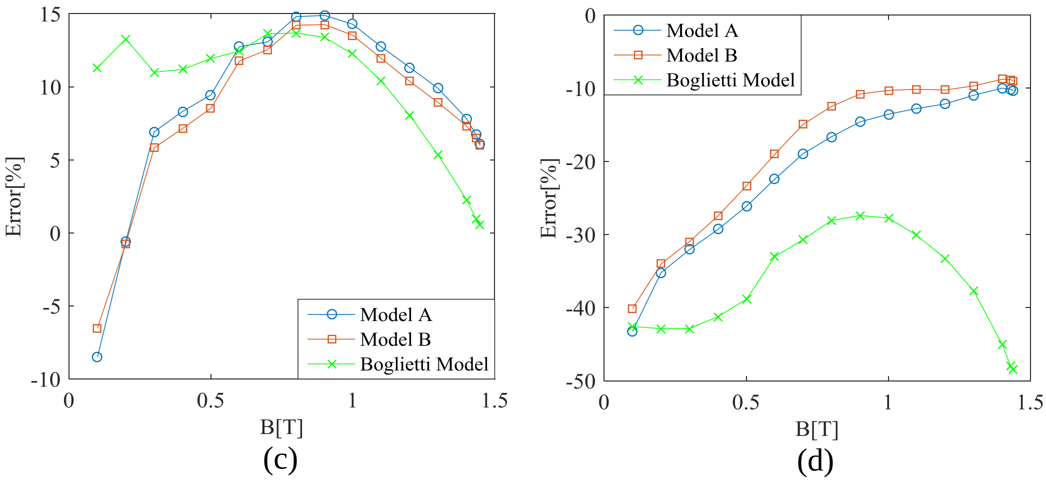

Fig. 9*: The relative error between predicted and measured losses as a function of flux density. Losses are predicted using time domain Model A, Model B, and Boglietti model with PWM waveform at f_{fun}=400 Hz and (a) Unipolar mode f_s=4k Hz (b) Bipolar mode f_s=4k Hz (c) Unipolar mode f_s=20k Hz (d) Bipolar mode f_s=20k Hz*

5. Summary and Conclusion

Three iron loss models have been used to predict the core losses in electrical steel laminations. The models, designated as Model A, Model B and the Boglietti Model are important due to their ubiquity and utility for predicting core losses in electromagnetic devices. The three models require parameter identification on the basis of sinusoidal loss measurements from Epstein frame experiments. Loss measurements were carried out for different magnetizing waveforms at various frequencies and induction levels. The accuracy and the applicability of the models were verified by comparing the measured losses to the computed values of losses. For non-sinusoidal waveforms that do not have minor loops, Model B and the Boglietti model predict losses with good accuracy at low, medium and high frequencies such as 50 Hz, 400 Hz and 1500 Hz, while Model A gives errors up to ~30% at low frequency.

Results for the PWM generated waveforms at fundamental frequency of 50 Hz show that Model B is accurate at low switching frequency (f_s of 500 Hz) with unipolar PWM. It is also reasonably accurate at low switching frequency with bipolar PWM, and for high switching frequency of 3 kHz with unipolar PWM. Model A is accurate at low fundamental (f_{fun}= 50 Hz) and low switching frequencies (f_s= 50 Hz and 500 Hz) in unipolar mode. Boglietti model is accurate at high switching frequency (f_s= 3 kHz) with unipolar PWM. In general, minor loops cause a deterioration in all three core loss model's accuracy, and this deterioration is most significant for the Boglietti model.

At a higher fundamental frequency of 400 Hz the following conclusions can be drawn. Model A and Model B predict losses at almost the same accuracy, under unipolar schemes for both low and high switching frequencies (f_s = 4 kHz and 20 kHz). In addition, Model A and Model B give accurate results for bipolar schemes at low switching frequency (f_s =4 kHz). With bipolar modes at high switching frequency (f_s =20 kHz), the relative errors of Model A and Model B exceed 20 %. The Boglietti model can predict losses accurately for unipolar modes at both 4 kHz and 20 kHz switching frequencies, while for bipolar mode the errors are above 25% at f_s =4 kHz, and are higher between 30% to 50% at 20 kHz.

Another observation is that the predicted losses using the Boglietti model are underestimated for unipolar schemes and overestimated for bipolar schemes.

6. Acknowledgment

This work was supported in part by the Automotive Partnership Canada (APC) program supported by the National Science and Engineering Research Council of Canada (NSERC).

7. References

[1] C. P. Steinmetz, "On the law of hysteresis," *American lnstitute of Elecfrical Engineers Transactions*, vol. 9, pp. 3-64, 1892.

[2] M. Popescu, T. J. E. Miller, M. McGilp, D. M. Ionel, S. J. Dellinger, and R. J. Heidemann, "On the Physical Basis of Power Losses in Laminated Steel and Minimum-Effort Modeling in an Industrial Design Environment," in *IEEE Industry Applications Conference, 2007. 42nd IAS Annual Meeting*, 2007, pp. 60-66.

[3] J. C. Akiror, "Model for Core Loss Prediction at High Frequency and High Flux Density," MSc Thesis, Department of Electrical and Computer Engineering, Concordia University, Montreal, Canada, 2012.

[4] M. Ibrahim and P. Pillay, "Advanced Testing and Modeling of Magnetic Materials Including a New Method of Core Loss Separation for Electrical Machines," *IEEE Transactions on Industry Applications*, vol. 48, pp. 1507-1515, 2012.

[5] E. Della Torre, "Problems in physical modeling of magnetic materials," *Physica B: Condensed Matter*, vol. 343, pp. 1-9, 1/1/ 2004.

[6] G. Bertotti, A. Canova, M. Chiampi, D. Chiarabaglio, F. Fiorillo, and A. M. Rietto, "Core loss prediction combining physical models with numerical field analysis," *Journal of Magnetism and Magnetic Materials*, vol. 133, pp. 647-650, 1994/05/01 1994.

[7] D. Eggers, S. Steentjes, and K. Hameyer, "Advanced Iron-Loss Estimation for Nonlinear Material Behavior," *IEEE Transactions on Magnetics*, vol. 48, pp. 3021-3024, 2012.

[8] V. Mănescu, G. Păltânea, and H. Gavrilă, "Hysteresis model and statistical interpretation of energy losses in non-oriented steels," *Physica B: Condensed Matter*, vol. 486, pp. 12-16, 4/1/ 2016.

[9] A. Krings, S. Nategh, A. Stening, H. Grop, O. Wallmark, and J. Soulard, "Measurement and Modeling of Iron Losses in Electrical Machines," presented at the Proceedings of the 5th International Conference Magnetism and Metallurgy WMM'12, Gent University, 2012.

[10] Z. Yu, N. Alatawneh, M. C. Cheng, and P. Pillay, "Magnetic core losses measurement instrumentations and a dynamic hysteresis loss model," in *Electrical Power & Energy Conference (EPEC), 2009 IEEE*, 2009, pp. 1-5.

[11] A. Krings and J. Soulard, "Overview and Comparison of Iron Loss Models for Electrical Machines," *Journal of Electrical Engineering*, vol. 10, no 3, pp. 162-169.

[12] *Direct-current Magnetic Measurements for Soft Magnetic Materials*: American Society for Testing and Materials . Committee A-6 on Magnetic Properties, 1970.

[13] G. S. Korzunin, V. K. Chistyakov, and F. F. Rimshev, "Developing techniques for testing magnetic properties of electric steels. I. Epstein’s apparatus (Review article)," *Russian Journal of Nondestructive Testing*, vol. 36, pp. 782-799, 2000.
[14] C. Appino, E. Ferrara, F. Fiorillo, L. Rocchino, C. Ragusa, J. Sievert, *et al.*, "International comparison on SST and Epstein measurements in grain-oriented Fe-Si sheet steel," *International Journal of Applied Electromagnetics & Mechanics*, vol. 48, pp. 123-133, 2015.
[15] G. Diaz, C. Gonzalez-Moran, P. Arboleya, and J. Gomez-Aleixandre, "Analytical Interpretation and Quantification of Rotational Losses in Stator Cores of Induction Motors," *IEEE Transactions on Magnetics*, vol. 43, pp. 3861-3867, 2007.
[16] N. Alatawneh and P. Pillay, "Rotational core loss measurements in clockwise and counterclockwise directions," in *Electrical Machines (ICEM), 2012 XXth International Conference on*, 2012, pp. 1412-1418.
[17] N. Alatawneh and P. Pillay, "The Minor Hysteresis Loop Under Rotating Magnetic Fields in Machine Laminations," *IEEE Transactions on Industry Applications*, vol. 50, pp. 2544-2553, 2014.
[18] M. Ibrahim, "Modeling of Core Losses in Electrical Machine Laminations Exposed to High Frequency and Non-sinusoidal Flux," MSc Thesis, Department of Electrical and Computer Engineering, Concordia University, Montreal, Canada, 2011.
[19] J. Reinert, A. Brockmeyer, and R. W. A. A. D. Doncker, "Calculation of losses in ferro- and ferrimagnetic materials based on the modified Steinmetz equation," *IEEE Transactions on Industry Applications*, vol. 37, pp. 1055-1061, 2001.
[20] L. Jieli, T. Abdallah, and C. R. Sullivan, "Improved calculation of core loss with nonsinusoidal waveforms," in *IEEE Industry Applications Society Annual Meeting*, 2001, pp. 2203-2210.
[21] A. Boglietti, A. Cavagnino, M. Lazzari, and M. Pastorelli, "Predicting iron losses in soft magnetic materials with arbitrary voltage supply: an engineering approach," *IEEE Transactions on Magnetics*, vol. 39, pp. 981-989, 2003.
[22] A. Boglietti, A. Cavagnino, D. M. Ionel, M. Popescu, D. A. Staton, and S. Vaschetto, "A General Model to Predict the Iron Losses in PWM Inverter-Fed Induction Motors," *IEEE Transactions on Industry Applications*, vol. 46, pp. 1882-1890, 2010.
[23] M. Popescu, D. M. Ionel, A. Boglietti, A. Cavagnino, C. Cossar, and M. I. McGilp, "A General Model for Estimating the Laminated Steel Losses Under PWM Voltage Supply," *IEEE Transactions on Industry Applications*, vol. 46, pp. 1389-1396, 2010.
[24] H. Jordan, "Die ferromagnetischen Konstanten für schwache Wechselfelder," *Elektrische Nachrichtentechnik*, vol. 1, pp. 7-29, 1924.
[25] D. M. Ionel, M. Popescu, M. I. McGilp, T. J. E. Miller, S. J. Dellinger, and R. J. Heideman, "Computation of Core Losses in Electrical Machines Using Improved Models for Laminated Steel," *IEEE Transactions on Industry Applications*, vol. 43, pp. 1554-1564, 2007.
[26] http://www.brockhaus.com/en/measurements/.
[27] F. J. G. Landgraf, "Nonoriented Electrical Steels," *The Journal of the Minerals*, vol. 64, pp. 764-771, 2012.
[28] IEC, "Methods of measurement of the magnetic properties of magnetically soft metallic and powder materials at frequencies in the range 20 Hz to 200 kHz by the use of ring specimens," *International Electrotechnical Commission (IEC) Standard Publication 60404-6, Geneva*, 2003.
[29] F. Fiorillo, *Measurement and Characterization of Magnetic Materials*: Elsevier Academic Press, 2004.

8. Appendix

Table 2 provides a summary of the accuracy of Model A, Model B, and Boglietti model with reference to the measured loss value for different waveforms and different frequencies. The following terms are used to evaluate the model's accuracy which are associated with a range of errors between measured and predicted loss value:

High (accuracy): **Errors ≤ ± 10%**

Moderate (accuracy): **± 10%< Errors ≤ ± 20%**

Low (accuracy): **± 20%<Errors ≤ ± 45%**

Poor (accuracy): **± 45%<Errors**

Table 2: Evaluation of Core Loss models' accuracy

<table>
<tr><th></th><th></th><th colspan="3">f [Hz]</th><th>Model A</th><th>Model B</th><th>Boglietti model</th></tr>
<tr><td rowspan="9">Non-sinusoidal waveform with no minor hysteresis loops</td><td rowspan="3">Triangular</td><td colspan="3">50</td><td>low</td><td>high</td><td>high</td></tr>
<tr><td colspan="3">300</td><td>high</td><td>high</td><td>high</td></tr>
<tr><td colspan="3">1500</td><td>high</td><td>high</td><td>high</td></tr>
<tr><td rowspan="3">Trapezoidal</td><td colspan="3">50</td><td>low</td><td>high</td><td>high</td></tr>
<tr><td colspan="3">300</td><td>high</td><td>high</td><td>high</td></tr>
<tr><td colspan="3">1500</td><td>high</td><td>high</td><td>high</td></tr>
<tr><td rowspan="3">Square</td><td colspan="3">50</td><td>low</td><td>high</td><td>high</td></tr>
<tr><td colspan="3">300</td><td>high</td><td>high</td><td>high</td></tr>
<tr><td colspan="3">1500</td><td>high</td><td>high</td><td>high</td></tr>
<tr><td></td><td colspan="4"></td><td colspan="3"></td></tr>
<tr><td></td><td colspan="2">f_{fun}[Hz]</td><td>f_s[Hz]</td><td>Scheme</td><td></td><td></td><td></td></tr>
<tr><td rowspan="8">Non-sinusoidal waveform with minor hysteresis loops PWM</td><td colspan="2" rowspan="4">50</td><td rowspan="2">500</td><td>UNI</td><td>moderate</td><td>high</td><td>low</td></tr>
<tr><td>BI</td><td>low</td><td>moderate</td><td>low</td></tr>
<tr><td rowspan="2">3 k</td><td>UNI</td><td>low</td><td>moderate</td><td>moderate</td></tr>
<tr><td>BI</td><td>poor</td><td>low</td><td>low</td></tr>
<tr><td colspan="2" rowspan="4">400</td><td rowspan="2">4 k</td><td>UNI</td><td>moderate</td><td>moderate</td><td>moderate</td></tr>
<tr><td>BI</td><td>high</td><td>high</td><td>low</td></tr>
<tr><td rowspan="2">20 k</td><td>UNI</td><td>moderate</td><td>moderate</td><td>high</td></tr>
<tr><td>BI</td><td>low</td><td>low</td><td>poor</td></tr>
</table>